

# Radiative lifetime and energy of the low-energy isomeric level in $^{229}\text{Th}$

E. V. Tkalya\*

*Skobeltsyn Institute of Nuclear Physics Lomonosov Moscow State University, Leninskie gory, Moscow 119991, Russia and  
Nuclear Safety Institute of Russian Academy of Science, Bol'shaya Tulsкая 52, Moscow 115191, Russia*

Christian Schneider, Justin Jeet, and Eric R. Hudson

*Department of Physics and Astronomy, University of California, Los Angeles, California 90095, USA*

(Dated: March 6, 2022)

We estimate the range of the radiative lifetime and energy of the anomalous, low-energy  $3/2^+$  ( $7.8 \pm 0.5$  eV) state in the  $^{229}\text{Th}$  nucleus. Our phenomenological calculations are based on the available experimental data for the intensities of  $M1$  and  $E2$  transitions between excited levels of the  $^{229}\text{Th}$  nucleus in the  $K^\pi[Nn_Z\Lambda] = 5/2^+[633]$  and  $3/2^+[631]$  rotational bands. We also discuss the influence of certain branching coefficients, which affect the currently accepted measured energy of the isomeric state. From this work, we establish a favored region where the transition lifetime and energy should lie at roughly the 90% confidence level. We also suggest new nuclear physics measurements, which would significantly reduce the ambiguity in the present data.

PACS numbers: 23.20.Lv, 21.10.Tg, 27.90.+b

## I. INTRODUCTION

The low-energy isomeric state in the  $^{229}\text{Th}$  nucleus is currently a subject of intense experimental and theoretical research (see a short review of the literature in [1, 2] and references below). This state is expected to provide access to a number of interesting physical effects, including the decay of the nuclear isomeric level via the electronic bridge mechanism in certain chemical environments [3–5], cooperative spontaneous emission [6] in a system of excited nuclei, the Mößbauer effect in the optical range [7], sensitive tests of the variation of the fine structure constant and the strong interaction parameter [8–11], a check of the exponentiality of the decay law of an isolated metastable state at long times [12], and accelerated  $\alpha$ -decay of the  $^{229}\text{Th}$  nuclei via the low energy isomeric state [13]. In addition, two applications that may have a significant technological impact were proposed: a new metrological standard for time [14] or the “nuclear clock” [15–18], and a nuclear laser (or gamma ray laser) in the optical range [7].

The ground state of the  $^{229}\text{Th}$  nucleus,  $J^\pi E = 5/2^+(0.0)$ , is the ground level of the rotational band  $K^\pi[Nn_Z\Lambda] = 5/2^+[633]$ . Currently, there is little doubt in the existence of the low-energy isomeric level  $J^\pi E = 3/2^+(E_{is})$ , which is the lowest level of the rotational band  $K^\pi[Nn_Z\Lambda] = 3/2^+[631]$ . The existence of the other levels of this band is reliably experimentally validated [1]. In addition, an independent corroboration of the existence of a low-lying state has been achieved experimentally in the reaction  $^{230}\text{Th}(d, t)^{229}\text{Th}$  [19]. This experiment provides strong evidence that the  $K^\pi[Nn_Z\Lambda] = 3/2^+[631]$  band head is located very close to the ground state, and, in fact, all available experimental data from these indi-

rect measurements of the  $J^\pi K[Nn_Z\Lambda] = 3/2^+3/2[631]$  isomeric state energy indicate that  $E_{is} < 10$  eV [20–23].

Unfortunately, the energy resolution of such experiments does not provide the accuracy required for direct optical spectroscopy of the nuclear isomeric  $M1$  transition  $5/2^+5/2[633](0.0) \leftrightarrow 3/2^+3/2[631](E_{is})$ , which is clearly a prerequisite for the aforementioned studies. Therefore, new approaches to determine the isomeric energy are required. While there are some ongoing attempts to better measure the isomeric transition energy (see for example [24]), directly driving the nuclear transition inside an insulator with a large band gap (i.e. a crystal), first proposed in the works [25, 26], or in sample of trapped ions [27–29] appear to be the most promising routes forward in the short term.

In the crystal approach, a band gap greater than  $E_{is}$  results in the absence of the conversion decay channel of the low energy isomeric state. Thus, the uncertainty in the decay probability, which is associated with electronic conversion, disappears. In Ref. [16, 30, 31] the requirements and characteristics of the requisite crystals were made rigorous, showing that  $^{229}\text{Th}:\text{LiCaAlF}_6$  and  $^{229}\text{Th}:\text{LiSrAlF}_6$  were likely good choices; other efforts focus on  $\text{CaF}_2$  [32, 33], or  $\text{ThF}_4$  and  $\text{Na}_2\text{ThF}_6$  [34]. Several experiments using this solid-state approach have been carried out in recent years [2, 24, 35], though as described in Sec. III, care must be taken to interpret the results of these experiments.

Experiments using trapped  $\text{Th}^+$  [29, 36] or  $\text{Th}^{3+}$  [28, 37–39] ions aim at exploiting the electronic bridge process [3–5], which can dominate the direct radiative decay of the isomeric transition. Using the electronic bridge process and exciting the isomeric transition in a multi-photon nucleon-electron simultaneous transition has the potential advantage of obviating the use of a vacuum ultraviolet laser system, at the expense of a modest increase in system complexity. Experiments have advanced rapidly in recent years and it is expected that with recent

\*Electronic address: [eugene.tkalya@mail.ru](mailto:eugene.tkalya@mail.ru)

high-resolution electronic spectra [36–38, 40], electronic bridge excitation rates can be better calculated in the near future.

In any experiment searching for the nuclear energy level, two key parameters in the preparation of the experiment are the isomeric state lifetime and energy. Therefore, the aim of this manuscript is to provide a critical assessment and estimation of these parameters to aid these experiments. In Section II of this paper, we analyze the experimental data on the nuclear matrix elements of transitions between states belonging to rotational bands  $K^\pi[Nn_Z\Lambda] = 5/2^+[633]$  and  $3/2^+[631]$  both in  $^{229}\text{Th}$  only and in comparable nuclei. In Section III, we estimate the radiative lifetime of the isomeric state using available experimental data for the transition rates of the interband  $M1$  and  $E2$  gamma transitions between excited levels of the  $^{229}\text{Th}$  nucleus. In Section IV we consider the importance of the conversion decay channel, showing that these processes will dominate the isomer radiative decay in cases where they are possible and, therefore, must be avoided. In Section V, we analyze the possible range of branching coefficients. We show how this range affects the determination of the isomeric energy in the experiments of Refs. [22, 41], which provide the currently accepted isomeric transition energy range. In Section VI, we briefly discuss the results of this work and present a “favored region”, which we recommend the community adopt in order to direct future searches. We conclude in Section VII with a summary of these results and point out new nuclear physics measurements that should be performed to considerably reduce the uncertainty in the present data.

In the present work, we use (if not noted otherwise) the following system of units:  $\hbar = c = 1$ .

## II. MATRIX ELEMENT OF THE ISOMERIC TRANSITION

Together with the energy of the isomeric level, the magnitude of the nuclear transition matrix element determines the half life  $T_{1/2}$  or the radiative lifetime  $\tau$  ( $\tau = T_{1/2}/\ln(2)$ ) of the isomeric state. Currently, there are two possibilities for phenomenological estimation of the reduced probability for the isomeric transition,  $B(M1; 3/2^+3/2[631] \rightarrow 5/2^+5/2[633])$ . The first possibility is to use parameters of the similar 311.9 keV transition in the spectrum of the  $^{233}\text{U}$  nucleus. The second is to take advantage of the available experimental data for the  $M1$  transitions between the rotational bands  $K^\pi[Nn_Z\Lambda] = 5/2^+[633]$  and  $3/2^+[631]$  in the excitation spectrum of the  $^{229}\text{Th}$  nucleus.

The first method can be motivated, because transitions  $3/2^+3/2[631] \rightarrow 5/2^+5/2[633]$  at 311.9 keV in the  $^{233}\text{U}$  nucleus and 7.8 eV in the  $^{229}\text{Th}$  nucleus look identical in terms of the rotational model and, in that context, should have the same reduced transition probabilities. (In this and the following section, we will

use the updated value of Ref. [41] for the  $^{229}\text{Th}$  isomeric energy,  $E_{is} = 7.8 \pm 0.5$  eV; see Section V for further discussion of the isomeric state energy.) The reduced probability of the transition in the  $^{233}\text{U}$  nucleus is known to be  $B_{W.u.}(M1; 3/2^+3/2[631](311.9 \text{ keV}) \rightarrow 5/2^+5/2[633](0.0)) = (0.33 \pm 0.05) \times 10^{-2}$  [42]. Here,  $B_{W.u.}$  denotes a reduced probability in Weisskopf units [43] (see Appendix A for details):

$$B_{W.u.}(M1; J_i \rightarrow J_f) = \frac{B(M1; J_i \rightarrow J_f)}{B(W; M1)}, \quad (1)$$

where  $B(W; M1) = (45/8\pi)\mu_N^2$  is the reduced probability of the nuclear  $M1$  transition in the Weisskopf model and  $\mu_N$  is the nuclear magneton.

Nonetheless, the  $^{233}\text{U}$  and  $^{229}\text{Th}$  nuclei are different and those differences could be crucial, which becomes evident when comparing to other nuclei with similar level structure. For example, a  $3/2^+3/2[631] \rightarrow 5/2^+5/2[633]$  transition with an energy of 221.4 keV also exists in the  $^{231}\text{Th}$  nucleus [44]. The half life of the  $3/2^+3/2[631](221.4 \text{ keV})$  state in  $^{231}\text{Th}$  is less than 74 ps and only one gamma transition, namely, the transition to the ground state has been observed experimentally from this level, with an internal conversion coefficient of 1.96 [44]. This is not surprising since according to the level scheme [44], the quantum numbers of states lying between the  $3/2^+3/2[631](221.4 \text{ keV})$  level and the ground state are such that the intensity of other possible transitions must be orders of magnitude smaller than the  $3/2^+3/2[631](221.4 \text{ keV}) \rightarrow 5/2^+5/2[633](0.0)$  transition. Therefore, the transition directly to the ground state should give the dominant contribution to the decay of the level in the  $^{231}\text{Th}$  nucleus, and the other decay channels cannot significantly change the lifetime of the level. Using the data from Ref. [44] the reduced probability of this transition in the  $^{231}\text{Th}$  nucleus is estimated as  $B_{W.u.}(M1; 3/2^+3/2[631](221.4 \text{ keV}) \rightarrow 5/2^+5/2[633](0.0)) \geq 0.93 \times 10^{-2}$ . This value is at least three times larger than would have been expected estimating it from the similar transition in  $^{233}\text{U}$ . Accordingly, interpolation from the  $^{233}\text{U}$  nucleus to the  $^{229}\text{Th}$  nucleus could lead to similar results. In addition, it is not obvious that measurements of the nuclear lifetimes,  $\gamma$ -ray intensities, the probabilities of electronic conversion, and other characteristics of this transition in the  $^{233}\text{U}$  nucleus are more accurate than for the  $^{229}\text{Th}$  nucleus, where measurement errors, as we shall see below, are significant.

For these reasons, we prefer to use the second approach to determine an estimate of  $B(M1; 3/2^+3/2[631](7.8 \text{ eV}) \rightarrow 5/2^+5/2[633](0.0))$ , which relies on available experimental data for the reduced probability of the  $M1$  transitions between the rotational bands  $K^\pi[Nn_Z\Lambda] = 5/2^+[633]$  and  $3/2^+[631]$  in the  $^{229}\text{Th}$  nucleus and the Alaga rules. Such a calculation assumes that the adiabatic condition is fulfilled (see [45] for a detailed analysis of the use of the adiabatic condition). Here, we do not consider the effects of nonadiabaticity because of the relatively large uncer-

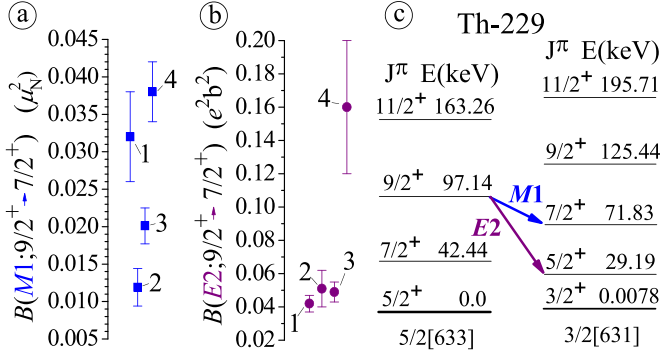


Figure 1: (color online). The experimental values for the reduced probability of the nuclear (a)  $9/2^+(97.14 \text{ keV}) \rightarrow 7/2^+(71.83 \text{ keV})$ , and (b)  $9/2^+(97.14 \text{ keV}) \rightarrow 5/2^+(29.19 \text{ keV})$  transitions. The relevant level scheme of the  $^{229}\text{Th}$  nucleus is shown in part (c). Data for the transitions were taken from: 1 – [46], 2 – [47], 3 – [48], and 4 – [49].

tainties and disagreements of the experimental data (see Fig. 1). Further, the well-expressed rotational structure of the bands in the  $^{229}\text{Th}$  nucleus and a number of other factors [45] allow us to neglect the Coriolis interaction for a preliminary estimation of the reduced probability of the isomeric transition from the experimental data for the  $9/2^+5/2[633](97.14 \text{ keV}) \rightarrow 7/2^+3/2[631](71.83 \text{ keV})$  transition in the  $^{229}\text{Th}$  nucleus. In this limit, we can, however, provide an estimate of the effect of the Coriolis interaction, which is quite small, on the matrix element [45].

Experimental data for  $B(M1; 9/2^+5/2[633](97.14 \text{ keV}) \rightarrow 7/2^+3/2[631](71.83 \text{ keV}))$  are, to our knowledge, available from four separate experiments [46–49]. As can be seen in Fig. 1, the reported values for the M1 transition show considerable spread. For comparison, in the case of the E2 transition, there is consensus between three of the measurements.

Using the Alaga rules, it is straightforward to obtain the reduced probability of the isomeric nuclear transition in terms of the measured M1 reduced probability:

$$B(M1; 3/2^+(7.8 \text{ eV}) \rightarrow 5/2^+(0.0)) = \frac{15}{7} B(M1; 9/2^+(97.14 \text{ keV}) \rightarrow 7/2^+(71.83 \text{ keV})).$$

The results of this calculation are shown in Table I for each measured value of  $B(M1; 9/2^+5/2[633](97.14 \text{ keV}) \rightarrow 7/2^+3/2[631](71.83 \text{ keV}))$  from Fig. 1(a).

Interestingly, the data of [48] affords another means to obtain  $B_{W.u.}(M1; 3/2^+(7.8 \text{ eV}) \rightarrow 5/2^+(0.0))$ . In that work, the relative intensities of the transitions from the level  $9/2^+3/2[631](125.44 \text{ keV})$  were also measured to states  $9/2^+(97.14 \text{ keV})$  and  $7/2^+(42.44 \text{ keV})$  of the  $5/2^+[633]$  rotational band. This allows us to calculate the reduced probabilities  $B(M1; 9/2^+3/2[631](125.44 \text{ keV}) \rightarrow 9/2^+5/2[633](97.14 \text{ keV})) = (0.56 \pm 0.25) \times 10^{-2} \mu_N^2$  and  $B(M1; 9/2^+3/2[631](125.44 \text{ keV}) \rightarrow$

Table I: Calculated reduced probabilities  $B_{W.u.}(M1; 3/2^+(7.8 \text{ eV}) \rightarrow 5/2^+(0.0))$  in  $^{229}\text{Th}$  based on  $B(M1; 9/2^+5/2[633](97.14 \text{ keV}) \rightarrow 7/2^+3/2[631](71.83 \text{ keV}))$  from given references.

| $B_{W.u.} (10^{-2})$ | based on  |
|----------------------|-----------|
| $3.83 \pm 0.72$      | Ref. [46] |
| $1.42 \pm 0.30$      | Ref. [47] |
| $2.41 \pm 0.29$      | Ref. [48] |
| $4.55 \pm 0.48$      | Ref. [49] |

Table II: Reduced probabilities  $B_{W.u.}(M1; 3/2^+3/2[631] \rightarrow 5/2^+5/2[633])$  for other nuclei or, for the case of  $^{229}\text{Th}$ , calculated from reduced probabilities of other transitions (see text).

| $B_{W.u.} (10^{-2})$ | nucleus           | from/based on |
|----------------------|-------------------|---------------|
| $0.33 \pm 0.05$      | $^{233}\text{U}$  | Ref. [42]     |
| $> 0.93$             | $^{231}\text{Th}$ | Ref. [44]     |
| $0.74 \pm 0.33$      | $^{229}\text{Th}$ | Ref. [48]     |

$7/2^+5/2[633](42.44 \text{ keV})) = (0.9 \pm 0.4) \times 10^{-3} \mu_N^2$  in the frame of the rotational model. Using the Alaga rules, we can then calculate the reduced probability of the M1(7.8 eV) isomeric transition. Both of the reduced probabilities give practically the same value  $B_{W.u.}(M1; 3/2^+(7.8 \text{ eV}) \rightarrow 5/2^+(0.0)) = (0.74 \pm 0.33) \times 10^{-2}$ . This result is shown in Table II along with the reduced probabilities of similar transitions in  $^{233}\text{U}$  at 311.9 keV and  $^{231}\text{Th}$  at 221.4 keV.

Thus, these estimates lead to a significant, more than an order of magnitude, range in the values for the reduced probability of the isomeric transition of the  $^{229}\text{Th}$  nucleus. However, if, for the aforementioned reasons, we restrict the estimate to those values calculated from the  $9/2^+5/2[633](97.14 \text{ keV}) \rightarrow 7/2^+3/2[631](71.83 \text{ keV})$  transitions the spread in mean values is within a factor of 3.

### III. RADIATIVE LIFETIME OF THE ISOMERIC LEVEL

Currently, the generally accepted value for the energy of the isomeric state  $3/2^+3/2[631]$  is  $7.8 \pm 0.5 \text{ eV}$  [22, 41]. Since the energy of the isomeric level exceeds, for example, the ionization potential of the isolated thorium atom, 6.08 eV, the radiative lifetime of the  $^{229}\text{Th}$  isomeric state is highly dependent on the chemical environment and electronic conversion is the dominant decay channel [3]. It is very difficult to directly observe the transition in such environments, as both the excitation radiation is absorbed by the electrons and the energy of any conversion electron is very small (only a few electron volts), making it difficult to detect. Similarly, it is difficult to predict the lifetime of the isomeric state for

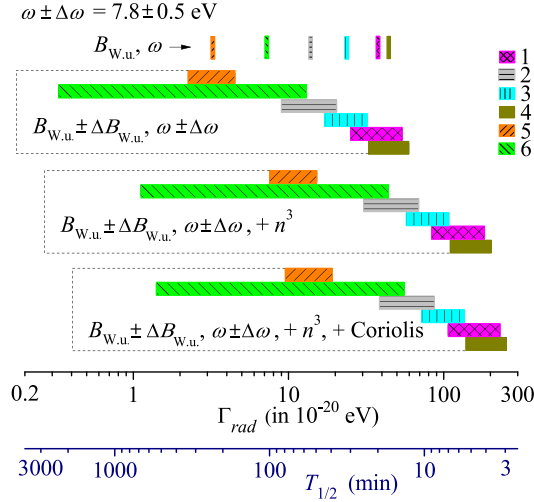


Figure 2: (color online). The range of possible radiative linewidths  $\Gamma_{rad}$  (upper scale) and half-lives  $T_{1/2}$  (lower scale) of the isomeric state  $3/2^+3/2[631](7.8 \pm 0.5 \text{ eV})$  in the  $^{229}\text{Th}$  nucleus. Calculations are based on values for  $B_{W.u.}(M1; 3/2^+3/2[631] \rightarrow 5/2^+5/2[633])$  from Tab. I (calculated from: 1 – [46], 2 – [47], 3 – [48], 4 – [49]) and, for completeness, Tab. II (5 – [42]; 6 – [48]). The refractive index  $n \approx 1.5$  increases the probability of the  $M1$  transition by a factor  $n^3$  (third row). The Coriolis interaction can lead to a slight increase of the linewidth by a factor of 1.2–1.3 [12] (fourth row).

thorium ions in the  $\text{Th}^{m+}$ ,  $m < 4$  charge state. Here, for example, the process of decay via the electronic bridge [3–5] can dominate, which cannot be calculated without precise knowledge of the nuclear transition energy and the wave functions of the valence electrons.

In the following, we only estimate the radiative half-life of the thorium isomeric state in the absence of any chemical effects based on the reduced probabilities discussed in Sec. II. As discussed previously, we prefer the four reduced probabilities calculated from the four measurements for the  $M1$   $9/2^+5/2[633](97.14 \text{ keV}) \rightarrow 7/2^+3/2[631](72.83 \text{ keV})$  transition in  $^{229}\text{Th}$  (see Tab. I), which appears most defensible, as this technique has shown to be accurate to within experimental error in cases where data exists [45]. Radiative half-lives based on the reduced probabilities from other transitions in  $^{229}\text{Th}$  or the similar transition in  $^{233}\text{U}$  are only given for completeness (see Tab. II). These results are directly applicable to trapped  $\text{Th}^{m+}$  ions with  $m \geq 4$  and, with a minor modification, to  $\text{Th}$  in a large-bandgap crystal. The modification in the latter case is due to the polarization of the dielectric medium and leads to a reduction of the half-life by a factor of  $1/n^3$  [25, 50], where  $n$  denotes the refractive index. The calculated half-lives can further be used in the trapped ion approach with  $m < 4$  to calculate e.g. the electron bridge process once the electronic spectra of the ions are known.

The results are shown in Fig. 2, first row, for  $\omega = 7.8 \text{ eV}$ . The range of half-lives including one standard

deviation in both the reduced probabilities and the currently accepted transition energy is given in the second row. The calculations for the case of a large-bandgap crystal with a typical refractive index  $n \approx 1.5$  is shown in the third row. Lastly, the additional inclusion of the Coriolis interaction leads to only a small correction (fourth row).

Using these results, we construct a favored region for the radiative half-life as a function of transition energy based only on the values for the reduced probabilities from Tab. I (see also Fig. 5 in Sec. VI). The center of this favored region is defined by the weighted average of the reduced probabilities. The bounds of the favored region are constructed as 1.96 standard deviations around the center of the favored region, which corresponds to roughly a 95% confidence level, however, considering that the individual reduced transition probabilities are not consistent within their errors, we increase the standard deviation by the Birge ratio of 3.4 [51]:

$$0.46 \times 10^6 \text{ s eV}^3/\omega^3 \leq T_{1/2} \leq 1.5 \times 10^6 \text{ s eV}^3/\omega^3.$$

Here, we did not include a crystal environment, as the inclusion of the refractive index  $n$  is straightforward. However, the small correction due to Coriolis interaction is included leading to an increase of the linewidth of the transition by a factor of 1.2–1.3 [45]. (These bounds are similar to those of Ref. [2], but we consider them more accurate as they include e.g. the Birge ratio.)

Alternatively, a more conservative region can be constructed which is bound by the extreme values of the individual radiative lifetimes deduced from Tab. I  $\pm 1.96$  standard deviations (see Fig. 5). Its functional form is given as (again including correction due to Coriolis interaction, but without crystal environment):

$$0.31 \times 10^6 \text{ s eV}^3/\omega^3 \leq T_{1/2} \leq 2.1 \times 10^6 \text{ s eV}^3/\omega^3.$$

#### IV. IMPORTANCE OF THE ELECTRONIC CONVERSION DECAY CHANNEL

As mentioned in Sec. III, the chemical environment can significantly affect the half-life of the isomeric state [3]. It most likely explains why, given the currently accepted value for the isomeric transition energy, that many previous experiments performed in powders, solids and solutions produced null results [52–56]; similarly, non-VUV sensitive measurements could have been affected by internal conversion [57, 58]. The internal conversion process could also have strong implications for the experiments reported in Refs. [24] and [35]. Though crystalline material is used as host in these experiments, the charge state of the thorium atom is not known, since the thorium atoms are either implanted into [24] or chemically adsorbed onto the surface of [35] the crystal. Therefore, it is likely that some, if not all, of the thorium atoms are in a local chemical environment that experiences electronic conversion. As we will see in the following, it is unlikely



the isomeric transition can be detected in such a system, if internal conversion is present. Thus, as aptly pointed out in Ref. [35], any conclusions drawn from experiments of this type should be considered preliminary until the thorium chemical environment is known.

If the energy of the isomeric level  $3/2^+3/2[631]$  in the  $^{229}\text{Th}$  exceeds the binding energy of electrons in the local chemical environment, the main channel of decay is electronic conversion [3]. Therefore, the lifetime of the isomeric state can be significantly reduced compared to the radiative lifetime only. In the following, we consider electronic conversion of the isomeric state in the neutral Th atom as an example to give a rough estimate of the lifetime for the  $^{229}\text{Th}$  isomeric state in such a chemical environment.

Electronic  $M1$  and  $E2$  conversion from the valence  $6d$  and  $7s$  shells of the thorium atom is possible for the nuclear isomeric transition. The ratio of radiation widths of the  $E2$  and  $M1$  transitions with energy of 7.8 eV in the  $^{229}\text{Th}$  nucleus is  $\Gamma_{\text{rad}}(W; E2)/\Gamma_{\text{rad}}(W; M1) \simeq 10^{-13}$  in the Weisskopf model, i.e. when the nuclear reduced probabilities are  $B_{W.u.}(M1) = 1$  and  $B_{W.u.}(E2) = 1$ . Therefore, we can neglect the  $E2$  contribution to the radiation width of the level for true values in the ranges  $B_{W.u.}(M1; 3/2^+(7.8 \text{ eV}) \rightarrow 5/2^+(0.0)) \simeq 10^{-1}$ – $10^{-3}$  and  $B_{W.u.}(E2; 3/2^+(7.8 \text{ eV}) \rightarrow 5/2^+(0.0)) \simeq 1$ – $10$ , respectively. As for the conversion decay channel, our calculations for the thorium atom give the relation  $\Gamma_{\text{conv}}(W; E2)/\Gamma_{\text{conv}}(W; M1) \simeq 10^{-6}$  in the Weisskopf model. Accordingly, for the true range of values for the reduced probabilities we find  $\Gamma_{\text{conv}}(E2)/\Gamma_{\text{conv}}(M1) \leq 10^{-3}$  for a transition with energy of 7.8 eV in the  $^{229}\text{Th}$  nucleus. Thus, we neglect the contribution of electronic  $E2$  conversion to the isomeric state conversion lifetime.

The calculation of the probability  $\Gamma_{\text{conv}}$  was performed using code developed in [59] on the basis of known code in [60], and then advanced in [3]. The calculated electronic  $M1$  conversion probability for the energy range 7.3 eV – 8.3 eV, using the reduced probabilities from Tables I and II, are presented in Figure 3. Taking into account the uncertainties on the magnitude of the nuclear matrix element of the transition, the characteristic lifetime of the isomer in an atom is  $\sim 10 \mu\text{s}$ . As a result, electronic conversion completely quenches the isomeric state non-radiatively. Thus, experiments looking for the emitted photons as a signal of the isomeric transition must ensure that the local chemical environment of the thorium atom does not support electronic conversion.

However, this is only one side of the issue. The  $M1$  isomeric transition like the other  $M1$  transitions between states of the bands  $K^\pi[Nn_Z\Lambda] = 5/2^+[633]$  and  $3/2^+[631]$ , is first-order forbidden by the asymptotic quantum numbers of the Nilsson model [61]. Indeed, we are considering  $M1$  transitions where  $\Delta K = 1$ ,  $\Delta N = 0$ ,  $\Delta n_Z = 0$ , and  $\Delta \Lambda = 2$ , while the selection rules for the  $M1$  transition allow the following change for the asymptotic quantum numbers for the case  $\Delta K = 1$ :  $\Delta N_a = 0, \pm 2$ ,  $\Delta n_{Z_a} = 0, \pm 1$ , and  $\Delta \Lambda_a = 0, \pm 1$  [61]

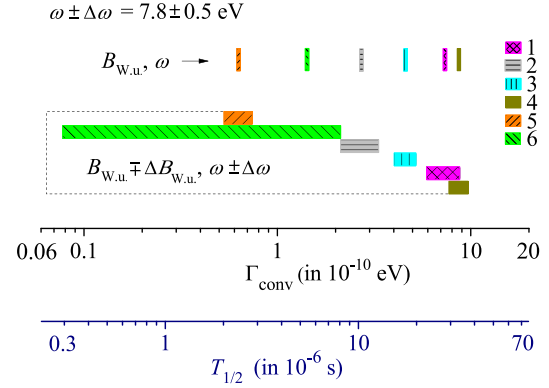


Figure 3: (color online). The ranges of possible conversion widths (the upper scale) and lifetimes (the lower scale) of the isomeric nuclear state in a neutral isolated Th atom. The designations are identical with designations in Fig. 2.

(the index  $a$  means “allowed”). Thus, the interband  $M1$  transitions  $K^\pi[Nn_Z\Lambda] = 5/2^+[633] \leftrightarrow 3/2^+[631]$  are weakly forbidden transitions by the number  $\Lambda$ . Phenomenology shows that the intensity of such  $M1$  interband transitions are weakened by a factor  $10^{-2n}$ , where  $n = |\Delta N_a - \Delta N| + |\Delta n_{Z_a} - \Delta n_Z| + |\Delta \Lambda_a - \Delta \Lambda|$  for  $K$ -allowed transitions. In our case  $n = 1$  and we can expect that such transitions have reduced probabilities  $B_{W.u.}(M1; 5/2^+[633] \leftrightarrow 3/2^+[631]) \simeq 10^{-2}$ .

The so-called anomalous internal conversion or the dynamic nuclear volume effect in internal conversion [62] is possible in transitions forbidden by the asymptotic selection rules. Its essence is as follows. Amplitudes of the electron wave functions for the  $ms_{1/2}$  ( $m = 1, 2, 3, \dots$ ) and  $lp_{1/2}$  ( $l = 2, 3, 4, \dots$ ) (or  $K$ ,  $L_{I,II}$ ,  $M_{I,II}, \dots$ ) shells inside the nucleus differ from zero:  $|\psi_{ms_{1/2}, lp_{1/2}}(0)| > 0$ . In internal conversion via these shells, the electron current effectively penetrates into the nucleus, and an “intranuclear” internal conversion becomes possible. The new phenomenon arises if the coordinates of the electron current  $j_e(r)$  and nuclear one  $J_N(R)$  satisfy the condition  $r < R < R_0$  (where  $R_0$  is a nuclear radius). In this case, the intranuclear matrix element is changed. The new nuclear matrix element is not forbidden by the asymptotic quantum numbers [63], and the intranuclear anomalous conversion becomes possible. Usually, intranuclear electron conversion is very small and amounts to  $(R_0/a_B)^3$ , where  $a_B$  is the Bohr radius, as compared with the usual internal conversion that is gained in the atomic shell outside the nucleus. But, in the case where the normal nuclear matrix element is forbidden by the asymptotic quantum numbers of the Nilsson model and anomalous intranuclear matrix element is allowed by the asymptotic quantum numbers, the smallness introduced by the function  $(R_0/a_B)^3$  is compensated since the factor  $10^{-2n}$  is absent for the anomaly, and anomalous internal conversion becomes observable.

In this sense, significant difference in the internal conversion coefficients with the  $M$  shell for the

$M1(29.19 \text{ keV})$  transitions in the  $^{229}\text{Th}$  nucleus, if they really exists, may indicate a strong anomaly. As aforementioned, the interband transition provides less than 10% of the total intensity of the 29.19 keV transitions. If this transition provides the observed difference in the internal conversion coefficients, the anomaly probably exists. And in this case, it will manifest itself in the conversion decay of the isomeric state  $3/2^+(7.8 \text{ eV})$ , because the  $7s_{1/2}$  shell is involved to the process. The amplitudes of course obey the condition  $\psi_{7s_{1/2}}(0) \ll \psi_{2s_{1/2}, 3s_{1/2}}(0)$ . However, the factor  $(\lambda_{is}/a_B)^2$ , where  $\lambda_{is} = 2\pi/E_{is}$ , is included in the formula for the probability of the dynamic effect of penetration [64], compensates the smallness of the amplitude of the  $7s_{1/2}$  wave function inside the nucleus. Thus, if the dynamic effect of penetration really exists in the  $M1$  interband transitions, it can also have an impact on the range of the lifetimes of the  $3/2^+(7.8 \text{ eV})$  isomer in the conversion decay.

Currently, we can only speculate of the possibility of anomalous internal conversion, since the accuracy of the measurements [47] were not sufficient. Therefore, it would be extremely useful if precise measurements of the internal conversion coefficients for interband magnetic dipole transitions between the bands  $K^\pi[Nn_Z\Lambda] = 5/2^+[633]$  and  $3/2^+[631]$  especially at the  $K$  and  $L$  atomic shells were performed.

## V. ENERGY OF THE NUCLEAR ISOMERIC LEVEL

The isomeric transition energy is equally as important as the isomeric transition radiative lifetime to current experiments. There have been several attempts [20, 21, 65] to infer the isomeric transition energy from indirect measurements of  $\gamma$ -ray transitions in the  $^{229}\text{Th}$  nucleus. Though the recommended value for the isomeric transition energy has changed considerably over the last 40 years, the consensus in the field is to accept the value put forward in Ref. [41] of  $E_{is} = 7.8 \pm 0.5 \text{ eV}$ , which updates a previous measurement by the same group [22] of  $E_{is} = 7.6 \pm 0.5 \text{ eV}$ . In the following, we detail the dependence of this value on the assumed branching ratios of interband  $E2$  transitions in the  $^{229}\text{Th}$  nucleus. We find there is considerable spread in the available experimental data, which could have significant affect on the interpretation of the data of Ref. [22].

In their original publication [22],  $\gamma$ -ray energies of four transitions consisting of a doublet at 29 keV and a doublet at 42 keV, respectively, were measured with a state-of-the-art microcalorimeter (see Fig. 4, solid arrows). In their analysis, they made use of the relation  $E_{is} = \Delta E_{29} - \Delta E_{42}$ , where  $\Delta E_{29}$  and  $\Delta E_{42}$  are the differences between the transition energies in the corresponding doublets, which reduces the dependency of the measurement on the absolute calibration of the detector. The authors accounted for an admixture of the low-intensity  $5/2^+3/2[631](29 \text{ keV}) \rightarrow 5/2^+5/2[633](0.0)$  transition

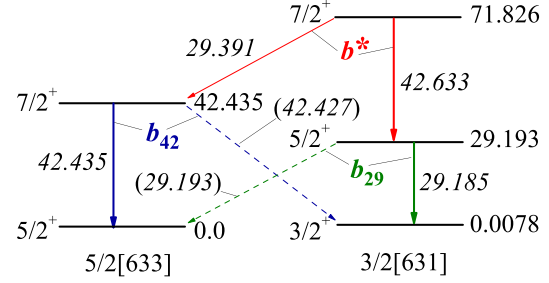


Figure 4: (color online). Relevant part of the level scheme of  $^{229}\text{Th}$  with transitions and branching ratios  $b^*$ ,  $b_{29}$ , and  $b_{42}$  used in the works [22, 41] to determine the energy of the isomeric level. Energies of the levels and transitions are given in keV.

(see Fig. 4, green dashed arrow) to their measured signal of the transition, which could not be resolved due to the energy resolution of the detector (26 eV). This admixture lead to a correction of  $\Delta E_{29} - \Delta E_{42} = 7.0 \pm 0.5 \text{ eV}$  to the value of the isomeric transition of  $E_{is} = 7.6 \pm 0.5 \text{ eV}$  [22]. Later, the authors included another unresolved weak interband transition,  $7/2^+5/2[633](42.435 \text{ keV}) \rightarrow 3/2^+3/2[631](7.8 \text{ eV})$  (see Fig. 4, blue dashed arrow), in their analysis, which shifted the isomeric transition energy to the currently accepted value of  $E_{is} = 7.8 \pm 0.5 \text{ eV}$  [41].

Specifically, the authors showed that the value of the isomeric transition energy is shifted due to the unresolved transitions by [41]

$$E_{is} = \frac{\Delta E_{29} - \Delta E_{42}}{1 - b_{29} - b_{42}}, \quad (2)$$

where the branching ratio  $b_{29}$  is given as [22]

$$b_{29} = \frac{\Gamma_{rad}^{tot}(29.193 \text{ keV})}{\Gamma_{rad}^{tot}(29.193 \text{ keV}) + \Gamma_{rad}^{tot}(29.185 \text{ keV})}, \quad (3)$$

and the branching ratio  $b_{42}$  is given as [41]

$$b_{42} = \frac{\Gamma_{rad}^{tot}(42.427 \text{ keV})}{\Gamma_{rad}^{tot}(42.427 \text{ keV}) + \Gamma_{rad}^{tot}(42.435 \text{ keV})}. \quad (4)$$

In order to determine  $b_{29}$ , the authors of Ref. [22] conducted additional measurements of the branching ratio

$$b^* = \frac{\Gamma_{rad}^{tot}(29.391 \text{ keV})}{\Gamma_{rad}^{tot}(29.391 \text{ keV}) + \Gamma_{rad}^{tot}(42.633 \text{ keV})} = \frac{1}{37} \quad (5)$$

with a quoted measurement accuracy of 8%. (Here,  $\Gamma_{rad}^{tot} = \Gamma_{rad}(M1) + \Gamma_{rad}(E2)$  and the designations of the transition energies correspond to those in Fig. 4.) Using the Alaga rules (see Appendix B) the authors obtained  $b_{29} \approx 1/13$ . This led to the aforementioned increase of the energy of isomeric transition by 0.6 eV in accordance with the Eq. (2). In Ref. [41], the authors performed an estimation of the value of the  $b_{42}$  coefficient, which is several times smaller (see in Tab. III) than  $b_{29}$ , leading to a

Table III: Branching ratios  $b_{29}$  and  $b_{42}$ . Results are based on the data of the given references.

| Ref.     | [22] | [41] | [46]  | [47]  | [48]  | [49]  |
|----------|------|------|-------|-------|-------|-------|
| $b_{29}$ | 1/13 |      | 1/3.5 | 1/7.8 | 1/5.0 | 1/3.1 |
| $b_{42}$ |      | 1/50 | 1/324 | 1/439 | 1/214 | 1/123 |

Table IV: Coefficients  $b^*$  and  $b_{29}$  obtained from the data for the relative intensities of transitions in [48].

| Decaying level | 7/2 <sup>+</sup> (71.826 keV) | 5/2 <sup>+</sup> (29.193 keV) |
|----------------|-------------------------------|-------------------------------|
| $b^*$          |                               | 1/17.5                        |
| $b_{29}$       |                               | 1/6.4                         |
|                |                               | 1/3.9                         |

smaller shift of 0.2 eV and the currently accepted value of  $E_{is} = 7.8 \pm 0.5$  eV.

Interestingly, the same branching ratios can be obtained from the experimental data [46–49] for parameters of interband (see in Figure 1(a) and (b)) and in-band transitions in the rotational bands 5/2<sup>+</sup>[633] and 3/2<sup>+</sup>[631] in the  $^{229}\text{Th}$  nucleus. The corresponding results are given in Table III, where the probabilities of the inband transitions were calculated using the internal quadrupole moment  $Q_{20}$  and the difference of the rotational and internal gyromagnetic ratio  $g_R$  and  $g_K$ , respectively (for the rotational band 5/2<sup>+</sup>[633] —  $Q_{20} = 7.1$  eb,  $|g_K - g_R| = 0.176$ ; for the rotational band 3/2<sup>+</sup>[631] —  $Q_{20} = 7.1$  eb,  $|g_K - g_R| = 0.56$ , (see [48])).

From Tab. III, it is obvious that the branching ratios calculated by the Alaga rules show considerable spread. This fact is relatively unimportant for the coefficient  $b_{42}$ , as the relatively small value given in [41] is the largest of the available in Table III. Thus, if, for example,  $b_{42} = 1/439$  the isomeric transition energy would effectively shift back to the previous result of  $E_{is} = 7.6 \pm 0.5$  eV [22]. The situation is more dramatic for the coefficient  $b_{29}$ . In the scenario  $b_{29} \approx 1/3.1$ , the energy of the isomer level would rise up to  $\sim 10.5$  eV.

The data from Ref. [48] allow for two additional estimates of the coefficient  $b_{29}$ . Specifically, Table VI of Ref. [48] presents the intensities of gamma transitions from the levels 7/2<sup>+</sup>(71.826 keV) and 5/2<sup>+</sup>(29.193 keV); some of these data are experimental results, while others (namely, the relative intensities of the interband transitions) were calculated from the strong coupling rotational model. The branching ratios calculated from these data are presented in Tab. IV. In the case of the data for decays from the 7/2<sup>+</sup>(71.826 keV) level, we calculated the branching ratio  $b_{29}$  by the formula (B4) using the coefficient  $b^*$ .

These branching ratios are in rough agreement with those calculated for Tab. III, but differ significantly from the measurement of Ref. [22]. The resolution of this tension between experiments is of the upmost importance. This can be seen by, for example, taking  $b_{29}$  to be given by the statistical average of the values calculated here.

In that case  $b_{29} = 1/5 \pm 1/10$  and the isomeric transition energy becomes  $E_{is} = 9.3 \pm 1.0$  eV. Despite this disagreement, we cannot reject the value of  $b_{29} = 1/13$  found in Ref. [22], since  $b^*$  is given directly from their experimental data and there is no proof this experiment, which used a state-of-the-art micro-calorimeter, is less reliable than the other measurements. Finally, we have performed Monte Carlo simulations of the Beck et al. experiments and if  $b_{29} = 1/3$ , an asymmetry in the 29 keV peak should be visible. Unfortunately, the size of this asymmetry is smaller than be confirmed by simply viewing the presented data in Ref. [22]. In this regard, it would be interesting to reanalyze the experimental data.

## VI. DEFINING A FAVORED AREA AND CURRENT EXCLUSIONS

As described in Sec. III, the measurements of Refs. [46–49] can be used to bound the isomeric level half life. In this section we will use the radiation *lifetime* instead of *half-life*, which is traditionally used in atomic spectroscopy. The radiative transition lifetime  $\tau$  is bounded by (roughly 95% confidence level)

$$0.66 \times 10^6 \text{ s eV}^3/\omega^3 \leq \tau \leq 2.2 \times 10^6 \text{ s eV}^3/\omega^3.$$

In Fig. 5, the bound is plotted as a function of isomeric transition energy (blue dash-dotted lines). For completeness, the energy ranges from 2.5 eV, which includes the now-rejected value of the transition energy from Ref. [20] with one standard deviation towards lower energies, up to 10.5 eV, which is expected to be the largest possible value for the transition energy based on Sec. V. Further, the energy range for the currently accepted value of the transition energy of Ref. [41] including two standard deviations is highlighted (see Fig. 5, blue dotted lines). The intersection of these two bounds, each at roughly the 95% confidence level, is marked as a blue shaded area and gives the primary region of interest. The energy and lifetime of the isomeric transition should be found at roughly the 90% confidence level in this region.

It is very likely that this region is somewhat conservative in its upper lifetime bound for two reasons. First, reduced transition probabilities calculated from the Alaga rules are typically smaller than actual values when the spin of the nucleus increases during the transition, as is the case here [67]. Second, the measurements of the  $B(M1; 9/2^+5/2[633](97.14 \text{ keV}) \rightarrow 7/2^+3/2[631](71.83 \text{ keV}))$  reduced transition probability rely on calculated values of the internal conversion coefficient, and there is evidence [68] that these calculated internal conversion coefficients may lead to an underestimate of the reduced probabilities by a factor of  $\sim 2$ .

Also shown in Fig. 5, are the results from both an indirect [66] and direct [2] search for the low energy isomeric transition in the  $^{229}\text{Th}$  nucleus; a similar measurement to [66] was also performed by [69]. In Ref. [66],  $^{229}\text{Th}$  produced in the  $\alpha$  decay of  $^{233}\text{U}$ , with an estimated 2% of

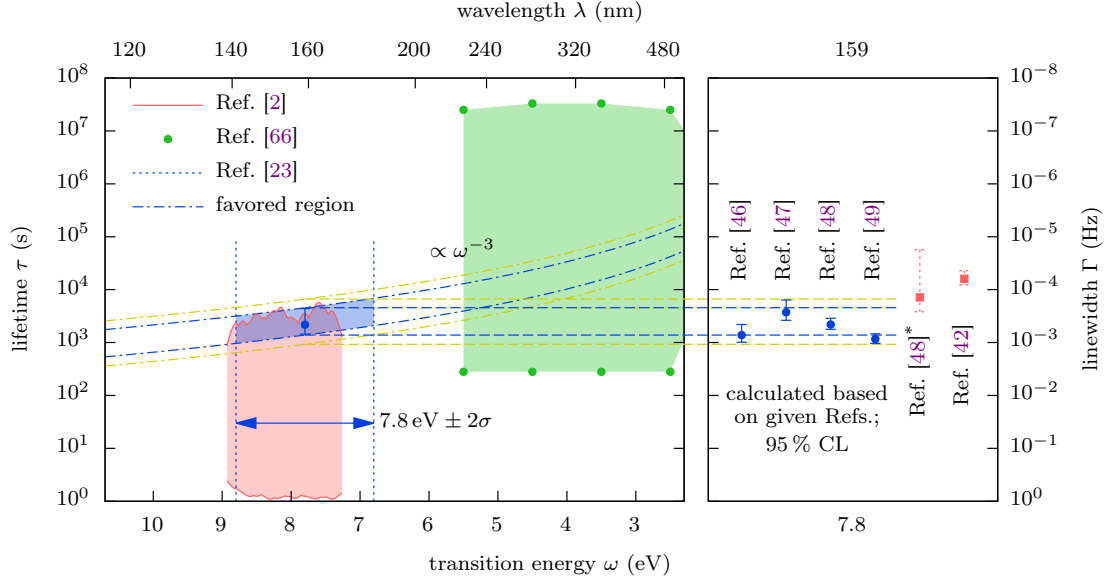


Figure 5: (color online). Favored region and experimentally excluded regions for the nuclear isomeric transition as a function of transition energy (wavelength) and radiative lifetime. (Left) The favored region (dash-dotted blue line; see text) and currently accepted energy of the isomeric transition (dotted blue lines) according to Ref. [23] are recommended as primary region of interest for current searches (blue shaded area). Experimentally excluded areas according to Ref. [66] (green shaded area between circles) and Ref. [2] (red shaded area between solid red lines) exclude parts of the favored region. Also shown are the more conservative bounds (outer dash-dotted yellow lines; see text). The point at 7.8 eV (blue circle) shows exemplarily the weighted average of the radiative lifetimes from reduced transition probabilities in Tab. I with 1.96 standard deviations including a Birge ratio of 3.4. (Right) Radiative lifetimes at 7.8 eV for individual values of the reduced transition probability with 1.96 standard deviations according to Tab. I (circles, blue) and Tab. II (squares, red). (The latter are only shown for completeness and do not enter into the construction of the favored region.)

the  $^{229}\text{Th}$  populating the isomeric state, is chemically isolated from the  $^{233}\text{U}$  and any resulting fluorescence monitored with a photomultiplier tube. The initial photon count rate, based on a chi-squared analysis of binned photon counts, is then compared to what is expected from the known starting amount of  $^{233}\text{U}$  which then sets limits on the isomer lifetime. From these results, a 99.7% confidence interval can be constructed that excludes the possibility of the transition existing with a certain lifetime in a given energy range, as depicted by the green shading in Fig. 5.

In the recent direct search [2], tunable, broadband, synchrotron radiation is used to illuminate a  $^{229}\text{Th}^{4+}$  doped  $\text{LiSrAlF}_6$  crystal. A photomultiplier tube is used to detect fluorescence subsequent to illumination of the crystal with the synchrotron beam. Applying a Feldman-Cousins analysis [70] to the binned photon counts, and comparing this to what is expected from experimental parameters, an exclusion region is created, depicted by the red shading between red solid lines in Fig. 5. This exclusion region represents a 90% confidence level for the absence of the isomeric transition.

## VII. RESULTS, DISCUSSION, AND REQUEST FOR FUTURE MEASUREMENTS

Even a cursory look at the results presented here reveals that the current situation is far from desirable. There is considerable scatter in the experimental data leading to a large range of predictions for the  $3/2^+(7.8\text{ eV})$   $^{229}\text{Th}$  isomer radiative lifetime. Likewise, though the basic value of  $\Delta E_{29} - \Delta E_{42} = 7.0 \pm 0.5\text{ eV}$  obtained in [22] is not currently in question, there is significant spread in the branching ratio of two unresolved transitions, which systematically shift the value of the isomeric state.

Of course, the situation could be made much less ambiguous with an improved measurement of the intensities of the gamma transitions and internal conversion coefficients between the rotational bands  $5/2^+[633]$  and  $3/2^+[631]$  in the  $^{229}\text{Th}$  nucleus. Such an experiment would ideally resolve the tension between the current results of Ref. [46–49]. This would allow accurate values of  $b_{29}$  and  $b_{42}$  to be calculated. Using these values in Eq. (2) and the value of  $\Delta E_{29} - \Delta E_{42} = 7.0 \pm 0.5\text{ eV}$  obtained in [22], which so far is not in question, the isomeric state energy could be found with greater certainty. Further, these same experiments would give a definitive means to calculate the nuclear matrix element of the iso-



meric transition, and thus the radiative lifetime of the isomeric state.

Ideally, the measurements should be conducted for transitions from the rotational band  $5/2^+[633]$  to the band  $3/2^+[631]$ , and vice versa, in the decay of states of the rotational band  $3/2^+[631]$ . Comparison of the data in Tables I and II indicates a systematic excess of the reduced probabilities obtained from the analysis of the decay data for the levels of the  $5/2^+[633]$  rotational band. Reduced probabilities of interband transitions from the rotational band  $3/2^+[631]$  to the band  $5/2^+[633]$  are considerably less. This may indicate an error of measurements, as well as the inapplicability of the adiabatic approximation in the calculation using the Alaga rules.

If performed, these measurements would considerably sharpen the region of interest that must be scanned in the search for the isomeric transition. Given the challenges faced by these searches, this sharpening of the search space may prove to be a prerequisite for the completion of this decades old quest.

## VIII. ACKNOWLEDGEMENT

This work has been supported in part by DARPA (QuASAR program), ARO (W911NF-11-1-0369), NSF (PHY-1205311), NIST PMG (60NANB14D302), and RCSA (20112810).

E.T. thanks the Russian government for its support of this work in the form of the salary of 22 thousand rubles per month (about \$ 340) and Moscow State University, which adds to the salary monthly else 50% of the specified amount.

## Appendix A: Weisskopf Units

In modern nuclear spectroscopy a value of the reduced probability of transition between the nuclear states with the spins  $I_i M_i$  and  $I_f M_f$

$$\begin{aligned} B(E/ML; i \rightarrow f) &= \sum_{M_f, M} |\langle I_f M_f | \hat{\mathcal{M}}_{LM}^{E/M} | I_i M_i \rangle|^2 \\ &= \frac{|\langle I_f | \hat{\mathcal{M}}_L^{E/M} | I_i \rangle|^2}{2I_i + 1}, \end{aligned} \quad (\text{A1})$$

where  $\langle I_f | \hat{\mathcal{M}}_L^{E/M} | I_i \rangle$  is the reduced matrix element of the transition operator  $\hat{\mathcal{M}}_{LM}^{E/M}$ , usually is expressed in the Weisskopf units; see Eq. (1) and Ref. [43]. The nuclear wave functions are as a rule so complex that an exact calculation of the nuclear matrix elements becomes very difficult. The simplified single-particle Weisskopf model is convenient because it makes it easy to evaluate the nuclear matrix element of the electromagnetic transition. For this purpose the model uses the proton single-particle radial wave functions of the form  $\varphi = \text{const.}$  inside the nucleus ( $R \leq R_0$ ) and  $\varphi(R) = 0$

outside the nucleus ( $R > R_0$ ). The normalization condition  $\int_0^{R_0} |\varphi(R)|^2 R^2 dR = 1$  gives  $\text{const.} = \sqrt{3/R_0^3}$ . Thus the total wave function of the proton has the form [43]

$$\Psi(\mathbf{R}) = \sqrt{\frac{3}{R_0^3}} Y_{LM}(\Omega_{\mathbf{R}}) \chi_{1/2} \quad \text{for } R \leq R_0, \quad (\text{A2})$$

where  $\chi_{1/2}$  is the spin part, and  $\Psi(\mathbf{R}) = 0$  for  $R > R_0$ .

The radial part of the matrix element of the  $EL$  proton transition operator  $\hat{\mathcal{M}}_{LM}^E = eR^L Y_{LM}(\Omega)$  is easily calculated with the wave functions (A2):

$$\langle \varphi_f(R) | R^L | \varphi_i(R) \rangle = \frac{3}{3+L} R_0^L.$$

From the angular part of the reduced matrix element in Eq. (A1),  $\langle f | Y_L(\Omega) | i \rangle$ , only a factor  $\sqrt{1/4\pi}$  is left, because  $\sqrt{(2L_i+1)(2L+1)} C_{L_i 0 L 0}^{L_f 0}$  with the factor  $1/\sqrt{(2I_i+1)}$  from (A1) gives a value of about 1. (Here  $C_{abcd}^{ef}$  is the Clebsch-Gordan coefficient [71].) As a result, the following expression is obtained in the Weisskopf model for the reduced probability of the  $EL$  single-particle transition

$$\begin{aligned} B(W; EL) &= \frac{e^2}{4\pi} \left( \frac{3}{3+L} \right)^2 R_0^{2L} \\ &= \frac{e^2}{4\pi} \left( \frac{3}{3+L} \right)^2 1.2^{2L} A^{2L/3} \text{ fm}^{2L}. \end{aligned}$$

Here, the value of  $R_0 = 1.2A^{1/3}$  fm was used for the radius of the nucleus with the atomic number  $A$ .

For the magnetic  $ML$  transition the orbital ( $l$ ) and the spin ( $\sigma$ ) contributions leads to the relation

$$\frac{|\hat{\mathcal{M}}_{LM}^M(l) + \hat{\mathcal{M}}_{LM}^M(\sigma)|^2}{|\hat{\mathcal{M}}_{LM}^E|^2} \simeq \frac{10}{(M_p R_0)^2} \quad (\text{A3})$$

between multipole moments of transition [43]. ( $M_p$  in Eq. (A3) is the proton mass.) This allows to write for the reduced probability of magnetic transitions in the Weisskopf model:

$$B(W; ML) = \frac{10}{(M_p R_0)^2} B(W; EL).$$

Now, one can express the real reduced probability of a nuclear transition,  $B(M/EL; i \rightarrow f)$ , through the single particle reduced probability of the Weisskopf model  $B(W; M/EL)$  according

$$B(E/ML; i \rightarrow f) = B(W; E/ML) B_{W.u.}(E/ML; i \rightarrow f),$$

where  $B_{W.u.}$  is the reduced probability in Weisskopf units, which is commonly used in tables of nuclear transitions.

The  $\gamma$  emission probability in the Weisskopf model [43]

$$\Gamma_{rad}(W; E/ML) = \frac{8\pi}{[(2L+1)!!]^2} \frac{L+1}{L} \omega^{2L+1} B(W; E/ML)$$

satisfies the condition

$$\frac{\Gamma_{rad}(W; L+1)}{\Gamma_{rad}(W; L)} \sim (\omega R_0)^2 \sim \left(\frac{R_0}{\lambda}\right)^2$$

for the emission of  $E(L+1)$  and  $EL$  (or  $M(L+1)$  and  $ML$ ) multipoles. This approximation is true if the nuclear radius  $R_0$  is small compared to the wavelength of nuclear transition  $\lambda$ . The latter condition is certainly satisfied for nuclear transitions with the energies up to several MeV.

## Appendix B: Branching Ratios

The section discussed the relation of the coefficients  $b^*$  and  $b_{29}$ . Simple algebraic transformation of the Eq. (5) enables us to express the ratio of the widths of the transitions with energies of 42.627 keV and 29.391 keV through coefficient  $b^*$ :

$$\frac{\Gamma_{rad}^{tot}(42.627 \text{ keV})}{\Gamma_{rad}^{tot}(29.391 \text{ keV})} = \frac{1 - b^*}{b^*} \quad (\text{B1})$$

Using the rotational model, we can express the radiation widths of the 29.185 keV transitions through the widths of the 42.627 keV transitions:

$$\begin{aligned} \Gamma_{rad}(M1; 29.185 \text{ keV}) &= \left( \frac{C_{5/23/210}^{3/23/2}}{C_{7/23/210}^{5/23/2}} \right)^2 \left( \frac{25.185}{42.627} \right)^3 \times \Gamma_{rad}(M1; 42.627 \text{ keV}) \\ &= 0.240 \Gamma_{rad}(M1; 42.627 \text{ keV}) \end{aligned}$$

and

$$\begin{aligned} \Gamma_{rad}(E2; 29.185 \text{ keV}) &= \left( \frac{C_{5/23/220}^{3/23/2}}{C_{7/23/220}^{5/23/2}} \right)^2 \left( \frac{25.185}{42.627} \right)^5 \times \Gamma_{rad}(E2; 42.627 \text{ keV}) \\ &= 0.241 \Gamma_{rad}(E2; 42.627 \text{ keV}). \end{aligned}$$

Due to the coincidental equality of the transformation coefficients for the  $M1$  and  $E2$  components we obtain

$$\Gamma_{rad}^{tot}(29.185 \text{ keV}) = 0.24 \Gamma_{rad}^{tot}(42.627 \text{ keV}). \quad (\text{B2})$$

Using the rotational model once again, we obtain the following relations:

$$\Gamma_{rad}(M1; 29.193 \text{ keV}) = 0.735 \Gamma_{rad}(M1; 29.391 \text{ keV})$$

and

$$\Gamma_{rad}(E2; 29.193 \text{ keV}) = 1.36 \Gamma_{rad}(E2; 29.391 \text{ keV}),$$

or, for the total linewidth,

$$\begin{aligned} \Gamma_{rad}^{tot}(29.193 \text{ keV}) &= 0.735 (\Gamma_{rad}^{tot}(29.391 \text{ keV}) \\ &\quad + 0.85 \Gamma_{rad}(E2; 29.391 \text{ keV})). \end{aligned}$$

Let us estimate the additional part  $0.85 \Gamma_{rad}(E2; 29.391 \text{ keV})$  to the width  $\Gamma_{rad}^{tot}(29.391 \text{ keV})$  using the mean values  $B(M1)$  and  $B(E2)$  for the interband transitions in Fig. 1 (a)–(b). The result is

$$\Gamma_{rad}(E2; 29.391 \text{ keV}) \simeq 2 \times 10^{-3} \Gamma_{rad}(M1; 29.391 \text{ keV}),$$

i.e. we really can neglect by the “extra” part  $0.85 \Gamma_{rad}(E2; 29.391 \text{ keV})$  in the width  $\Gamma_{rad}^{tot}(29.391 \text{ keV})$  and use the estimation

$$\Gamma_{rad}^{tot}(29.193 \text{ keV}) \approx 0.735 \Gamma_{rad}^{tot}(29.391 \text{ keV}). \quad (\text{B3})$$

Substituting expression (B2), (B3) and (B1) in (3) we finally obtain

$$\begin{aligned} b_{29} &= \left( 1 + \frac{0.24 \Gamma_{rad}^{tot}(42.627 \text{ keV})}{0.735 \Gamma_{rad}^{tot}(29.193 \text{ keV})} \right)^{-1} \\ &= \left( 1 + \frac{0.24}{0.735} \frac{1 - b^*}{b^*} \right)^{-1}. \end{aligned} \quad (\text{B4})$$

- [1] E. Browne and J. K. Tuli, Nucl. Data Sheet **109**, 2657 (2008).
- [2] J. Jeet, C. Schneider, S. T. Sullivan, W. G. Rellergert, S. Mirzadeh, A. Cassanho, H. P. Jenssen, E. V. Tkalya, and E. R. Hudson, Phys. Rev. Lett. **114**, 253001 (2015).
- [3] V. F. Strizhov and E. V. Tkalya, Sov. Phys. JETP **72**, 387 (1991).
- [4] S. G. Porsev and V. V. Flambaum, Phys. Rev. A **81**, 032504 (2010).
- [5] S. G. Porsev and V. V. Flambaum, Phys. Rev. A **81**, 042516 (2010).
- [6] R. H. Dicke, Phys. Rev. **93**, 99 (1954).
- [7] E. V. Tkalya, Phys. Rev. Lett. **106**, 162501 (2011).
- [8] V. V. Flambaum, Phys. Rev. Lett. **97**, 092502 (2006).
- [9] H.-t. He and Z.-z. Ren, J. Phys. G: Nucl. Phys. **34**, 1611

- (2007).
- [10] A. C. Hayes and J. L. Friar, Phys. Lett. B **650**, 229 (2007).
- [11] E. Litvinova, H. Feldmeier, J. Dobaczewski, and V. Flambaum, Phys. Rev. C **79**, 064303 (2009), URL <http://link.aps.org/doi/10.1103/PhysRevC.79.064303>.
- [12] A. M. Dykhne and E. V. Tkalya, JETP Lett. **67**, 549 (1998).
- [13] A. M. Dykhne, N. V. Eremin, and E. V. Tkalya, JETP Lett. **64**, 345 (1996).
- [14] E. V. Tkalya, V. O. Varlamov, V. V. Lomonosov, and S. A. Nikulin, Phys. Scr. **53**, 296 (1996).
- [15] E. Peik and C. Tamm, Europhys. Lett. **61**, 181 (2000).
- [16] W. G. Rellergert, D. DeMille, R. R. Greco, M. P. Hehlen, J. R. Torgerson, and E. R. Hudson, Phys. Rev. Lett. **104**,

- 200802 (2010).
- [17] C. J. Campbell, A. G. Radnaev, A. Kuzmich, V. A. Dzuba, V. V. Flambaum, and A. Derevianko, *Phys. Rev. Lett.* **108**, 120802 (2012).
  - [18] E. Peik and M. Okhapkin, *C. R. Phys.* **16**, 516 (2015), ISSN 1631-0705, URL <http://www.sciencedirect.com/science/article/pii/S1631070515000213>.
  - [19] D. G. Burke, P. E. Garrett, T. Qu, and R. A. Naumann, *Nucl. Phys. A* **809**, 129 (2008).
  - [20] R. G. Helmer and C. W. Reich, *Phys. Rev. C* **49**, 1845 (1994).
  - [21] Z. O. Guimaraes-Filho and O. Helene, *Phys. Rev. C* **71**, 044303 (2005).
  - [22] B. R. Beck, J. A. Becker, P. Beiersdorfer, G. V. Brown, K. J. Moody, J. B. Wilhelmy, F. S. Porter, C. A. Kilbourne, and R. L. Kelley, *Phys. Rev. Lett.* **98**, 142501 (2007).
  - [23] B. R. Beck, C. Y. Wu, P. Beiersdorfer, G. V. Brown, J. A. Becker, J. K. Moody, J. B. Wilhelmy, F. S. Porter, C. A. Kilbourne, and R. L. Kelley, Lawrence Livermore National Laboratory, Conference LLNL-PROC-415170, 2009, URL <http://www.osti.gov/scitech/biblio/964521-r2Qnkb/#.>
  - [24] X. Zhao, Y. N. M. de Escobar, R. Rundberg, E. M. Bond, A. Moody, and D. J. Vieira, *Phys. Rev. Lett.* **109**, 160801 (2012).
  - [25] E. V. Tkalya, *JETP Lett.* **71**, 311 (2000).
  - [26] E. V. Tkalya, A. N. Zherikhin, and V. I. Zhudov, *Phys. Rev. C* **61**, 064308 (2000).
  - [27] W. Kälber, J. Rink, K. Bekt, W. Faubel, S. Göring, G. Meisel, H. Rebel, and R. Thompson, *Z. Phys. A* **334**, 103 (1989), ISSN 0939-7922, URL <http://dx.doi.org/10.1007/BF01294392>.
  - [28] C. J. Campbell, A. V. Steele, L. R. Churchill, M. V. DePalatis, D. E. Naylor, D. N. Matsukevich, A. Kuzmich, and M. S. Chapman, *Phys. Rev. Lett.* **102**, 233004 (2009).
  - [29] O. A. Herrera-Sancho, M. V. Okhapkin, K. Zimmermann, C. Tamm, E. Peik, A. V. Taichenachev, V. I. Yudin, and P. Glowacki, *Phys. Rev. A* **85**, 033402 (2012).
  - [30] W. G. Rellergert, S. T. Sullivan, D. DeMille, R. R. Greco, M. P. Hehlen, R. A. Jackson, J. R. Torgerson, and E. R. Hudson, *IOP Conf. Ser.: Mater. Sci. Eng.* **15**, 012005 (2010).
  - [31] M. P. Hehlen, R. R. Greco, W. G. Rellergert, S. T. Sullivan, D. DeMille, R. A. Jackson, E. R. Hudson, and J. R. Torgerson, *J. Lumin.* **133**, 91 (2013).
  - [32] P. Dessoic, P. Mohn, R. A. Jackson, J. Winkler, M. Schreidl, G. Kazakov, and T. Schumm, *J. Phys.: Condens. Matter* **26**, 105402 (2014).
  - [33] S. Stellmer, M. Schreidl, and T. Schumm, *arXiv* **1506.01938**, 1 (2015), 1506.01938, URL <http://arxiv.org/abs/1506.01938v1>.
  - [34] J. K. Ellis, X.-D. Wen, and R. L. Martin, *Inorg. Chem.* **53**, 6769 (2014).
  - [35] A. Yamaguchi, M. Kolbe, H. Kaser, T. Reichel, A. Gottwald, and E. Peik, *New J. Phys.* **17**, 053053 (2015).
  - [36] M. V. Okhapkin, D. M. Meier, E. Peik, M. S. Safronova, M. G. Kozlov, and S. G. Porsev, *Phys. Rev. A* **92**, 020503(R) (2015).
  - [37] C. J. Campbell, A. G. Radnaev, and A. Kuzmich, *Phys. Rev. Lett.* **106**, 223001 (2011).
  - [38] A. G. Radnaev, C. J. Campbell, and A. Kuzmich, *Phys. Rev. A* **44**, 060501(R) (2012).
  - [39] K. Bely, *Phys. Rev. Lett.* **112**, 062503 (2014).
  - [40] O. A. Herrera-Sancho, N. Nemitz, M. V. Okhapkin, and E. Peik, *Phys. Rev. A* **88**, 012512 (2013), URL <http://link.aps.org/doi/10.1103/PhysRevA.88.012512>.
  - [41] B. R. Beck and J. A. Becker and P. Beiersdorfer and G. V. Brown and K. J. Moody and J. B. Wilhelmy and F. S. Porter and C. A. Kilbourne and R. L. Kelley, Report LLNL-PROC-415170., URL <https://e-reports-ext.llnl.gov/pdf/375773.pdf>.
  - [42] B. Singh and J. K. Tuli, *Nucl. Data Sheet* **105**, 109 (2005).
  - [43] J. M. Blatt and V. F. Weisskopf, *Theoretical Nuclear Physics*. John Wiley & Sons, Inc. NY, 1952.
  - [44] E. Browne and J. K. Tuli, *Nucl. Data Sheet* **114**, 751 (2013).
  - [45] A. M. Dykhne and E. V. Tkalya, *JETP Lett.* **67**, 251 (1998).
  - [46] J. C. E. Bemis, F. K. McGowan, J. J. L. C. Ford, W. T. Milner, R. L. Robinson, P. H. Stelson, G. A. Leander, and C. W. Reich, *Phys. Scr.* **38**, 657 (1988).
  - [47] K. Gulda et al., (ISOLDE Collaboration), *Nucl. Phys. A* **703**, 45 (2002).
  - [48] V. Barci, G. Ardisson, G. Barci-Funel, B. Weiss, O. El Samad, and R. K. Sheline, *Phys. Rev. C* **68**, 034329 (2003).
  - [49] E. Ruchowska, W. A. Plociennik, J. Zylicz, et al., *Phys. Rev. C* **73**, 044326 (2006).
  - [50] G. L. J. A. Rikken and Y. A. R. R. Kessener, *Phys. Rev. Lett.* **74**, 880 (1995).
  - [51] O. Bodnar and C. Elster, *Metrologia* **51**, 516 (2014).
  - [52] E. Browne, E. B. Norman, R. D. Canaan, D. C. Glasgow, J. M. Keller, and J. P. Young, *Phys. Rev. C* **164**, 014311 (2001).
  - [53] H. Kikunaga, Y. Kasamatsu, H. Haba, T. Mitsugashira, M. Hara, K. Takamiya, T. Ohtsuki, A. Yokoyama, T. Nakanishi, and A. Shinohara, *Phys. Rev. C* **80**, 034315 (2009), URL <http://link.aps.org/doi/10.1103/PhysRevC.80.034315>.
  - [54] T. Mitsugashira, M. Hara, T. Ohtsuki, H. Yuki, K. Takamiya, Y. Kasamatsu, A. Shinohara, H. Kikunaga, and T. Nakanishi, *J. Radioanal. Nucl. Chem.* **255**, 63 (2003), ISSN 0236-5731, URL <http://dx.doi.org/10.1023/A:3A1022267428310>.
  - [55] K. Zimmermann, Dr. rer. nat., Gottfried Wilhelm Leibniz Universität Hannover (2010), URL <http://edok01.tib.uni-hannover.de/edoks/e01dh10/634991264.pdf>.
  - [56] E. L. Swanberg Jr., Dissertation, University of California, Berkeley (2012), URL [http://digitalassets.lib.berkeley.edu/etd/ucb/text/Swanberg\\_berkeley\\_0028E\\_12982.pdf](http://digitalassets.lib.berkeley.edu/etd/ucb/text/Swanberg_berkeley_0028E_12982.pdf).
  - [57] S. B. Utter, P. Beiersdorfer, A. Barnes, R. W. Loughheed, J. R. Crespo López-Urrutia, J. A. Becker, and M. S. Weiss, *Phys. Rev. Lett.* **82**, 505 (1999), URL <http://link.aps.org/doi/10.1103/PhysRevLett.82.505>.
  - [58] R. W. Shaw, J. P. Young, S. P. Cooper, and O. F. Webb, *Phys. Rev. Lett.* **82**, 1109 (1999), URL <http://link.aps.org/doi/10.1103/PhysRevLett.82.1109>.
  - [59] A. A. Soldatov and D. P. Grechukhin, Kurchatov Institute of Atomic Energy Report-3174, Moscow, 1979.
  - [60] I. M. Band and V. I. Fomichev, *At. Data Nucl. Data Tabl.* **23**, 295 (1979).
  - [61] S. G. Nilsson, *Mat.-fys medd. danske selskab* **Bd. 29**, n. 16 (1955).

- [62] E. L. Church and J. Weneser, Phys. Rev. **104**, 1382 (1956).
- [63] M. E. Voikhansky, M. A. Listengarten, and I. M. Band, Penetration effects in internal conversion. In: *Internal Conversion Processes*, Ed. by J.H. Hamilton, Academic Press, NY, 1966, p.581.
- [64] E. V. Tkalya, JETP Lett. **78**, 239 (1994).
- [65] C. W. Reich and R. G. Helmer, Phys. Rev. Lett. **64**, 271 (1990).
- [66] I. Moore, I. Ahmad, K. Bailey, D. L. Bowers, Z.-T. Lu, T. P. O'Connor, and Z. Yin, Argonne National Laboratory, Physics Division Report No. PHY-10990-ME-2004, 2004, URL [http://www.phy.anl.gov/mep/atta/publications/thorium229\\_phy-10990-me-2004.pdf](http://www.phy.anl.gov/mep/atta/publications/thorium229_phy-10990-me-2004.pdf).
- [67] R. Casten, *Nuclear Physics from a Simple Perspective* (Oxford University Press, 2000).
- [68] E. F. Tret'yakov, M. P. Anikina, L. L. Gol'din, G. I. Novikova, and N. I. Pirogova, Sov. Phys. JETP **37**, 656 (1960).
- [69] Y. Kasamatsu, H. Kikunaga, K. Nakashima, K. Takamiya, T. Mitsugashira, T. Nakanishi, T. Ohtsuki, H. Yuki, W. Sato, and A. Shinohara, Research Report vol. 38, p. 32–35, Laboratory of Nuclear Science, Tohoku University (2005), URL <http://www.lns.tohoku.ac.jp/fy2011/research/report/2005/2005.htm>.
- [70] G. J. Feldman and R. D. Cousins, Phys. Rev. D **57**, 3873 (1998), URL <http://link.aps.org/doi/10.1103/PhysRevD.57.3873>.
- [71] D. A. Varshalovich, A. N. Moskalev, and V. K. Khersonskii, *Quantum Theory of Angular Momentum* (World Scientific Publ., London, 1988).